Applied Physics Letters

Quantum size effect in nanocorrals: From fundamental to potential applications

Cite as: Appl. Phys. Lett. **117**, 060501 (2020); https://doi.org/10.1063/5.0015542
Submitted: 29 May 2020 . Accepted: 01 July 2020 . Published Online: 10 August 2020

Qili Li, Rongxing Cao, and Haifeng Ding

Applied Physics Letters PERSPECTIVE scitation.org/journal/apl

Quantum size effect in nanocorrals: From fundamental to potential applications

Cite as: Appl. Phys. Lett. **117**, 060501 (2020); doi: 10.1063/5.0015542
Submitted: 29 May 2020 · Accepted: 1 July 2020 ·
Published Online: 10 August 2020

Qili Li,[1] Rongxing Cao,[1,2] and Haifeng Ding[1,3,a)]

AFFILIATIONS

[1]National Laboratory of Solid State Microstructures and Department of Physics, Nanjing University, Nanjing 210093, China
[2]College of Physics Science and Technology, Yangzhou University, Yangzhou 225002, China
[3]Collaborative Innovation Center of Advanced Microstructures, Nanjing 210093, China

[a)]**Author to whom correspondence should be addressed:** hfding@nju.edu.cn

ABSTRACT

Conventional silicon-based devices are approaching the scaling limits toward super miniaturization, where the quantum size effect naturally emerges with increasing importance. Exploring the quantum size effect may provide additional functionality and alternative architectures for information processing and computation. Scanning tunneling microscopy/spectroscopy is an ideal tool to explore such an opportunity as it can construct the devices in an atom-by-atom fashion and investigate their morphologies and properties down to the atomic level. Utilizing nanocorrals as examples, the quantum size effect is demonstrated to possess the great capability in guiding the adatom diffusion and the self-assembly, controlling the statistical fluctuation, tuning the Kondo temperature, etc. Besides these fundamentals, it also shows strong potential in logic operations as the basic logic gates are constructed.

In the past several decades, the semiconductor industry had a fast development along the guideline of Moore's law. Generally, the number of transistors on a microprocessor chip doubled every two years. Nowadays, conventional silicon-based devices are approaching the scaling limits toward super miniaturization.[1] With decreasing the device size, one of the well-known phenomena, the quantum size effect (QSE) naturally evolves with increasing importance. The QSE describes a system whose size is comparable with the effective de Broglie wavelength of the carriers, resulting in the size quantization of the energy of the carriers.[2] Exploring the QSE may provide additional functionality and alternative architectures for information processing and computation.

Generally, the QSE can be classified into three categories according to the number of dimensions in size quantization: (i) one-dimensionally (1D) confined ultrathin films; (ii) 2D confined nanocorrals and islands; and (iii) 3D confined quantum dots. The experimental exploration of the 1D-QSE in thin films can be dated to 1966, where the thickness dependences of the resistivity, Hall coefficient, magnetoresistance, and tunnel spectroscopy were observed in thin bismuth films.[3,4] From then on, the QSE in thin films was also extended to the investigation of optical phenomena, phase transitions, superconductivity, magnetism, etc.[2,5] Toward application, the QSE in ultrathin films is able to tune the coupling between magnetic layers and control giant magnetoresistance.[6,7] For the 3D-QSE in quantum dots, it arose in the late 1980s[8] and has been booming fast since then. Quantum dots have been widely used for medical and display applications[9] and also exhibit great potential in multiple applications such as solar harvesting,[10] flexible nonvolatile memory,[11] and energetic material.[12] Moreover, quantum dots are also an alternative architecture toward the quantum computation.[13] With regard to the 2D-QSE, it is the mostly related QSE to the super miniaturization where the lateral confinement is dominant.

Here, we focus our discussion on the 2D-QSE with nanocorrals (Fig. 1) created by atom manipulation[14] since the investigation can be made in a designed manner. Besides the pioneering works showing the quantum confinement of the electronic states[15] and projecting the Kondo resonance of one focal point of the ellipses to the other focal point (quantum mirage effect),[16] the QSE is also used in modulating the atom diffusion, guiding the self-assembly,[17] controlling the statistical fluctuation,[18] and tuning the Kondo temperature.[19] A latest work demonstrates that non-Kondo effect based quantum mirages can exist in a wide energy range beyond the Fermi level.[20] What is more, the signal of the Kondo-free mirage can be even stronger than that of the object. With these merits, the manipulation of Kondo-free mirages is exploited to realize basic logic operations, such as NOT, FANOUT, and OR gates.[20]

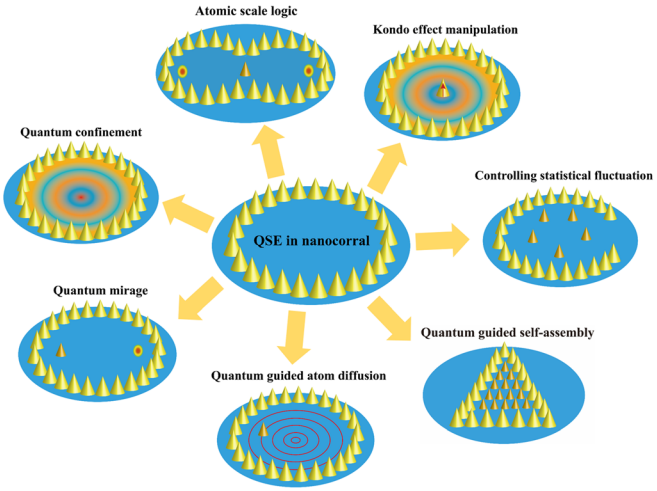

FIG. 1. Sketch of the quantum size effect in nanocorrals and their fields of exploration.

Lateral confined electronic surface states introduced by the molecular network[21,22] or parallel atomic/molecular chains[23,24] have been shown to substantially affect the atomic motion behavior on the surface. Recently, inspired by the theoretical prediction,[25] quantum guided atomic diffusion and self-assembly have also been experimentally demonstrated inside the nanocorrals.[17] Utilizing the Fe corrals constructed by atom manipulation and subsequently deposited Gd atoms on the Ag(111) surface, the statistics on the Gd adatom diffusion inside the corral has been harvested from hundreds of consecutive scanning tunneling microscopy (STM) images. Three concentric preferential orbits of adatom motion plus one preferred location at the center can be observed in the cumulative image [Fig. 2(a)]. We note that the brighter spots with much higher occupation probability on the outermost orbit can be attributed to the geometric deviation of the constructed nanocorral from the perfect circular shape.[17] The orbital separation of ~3.8 nm is consistent with half of the Fermi wavelength of the Ag(111) surface. This probability distribution is closely related to the characteristic electronic standing-wave patterns induced by the QSE,[15,17] while in sharp contrast to the random walk on a flat terrace free of nanocorrals.[23] The same conclusion was also confirmed in other different sized nanocorrals.[26] These experimental findings demonstrate that lateral quantum confinement can be used to engineer atom diffusion.

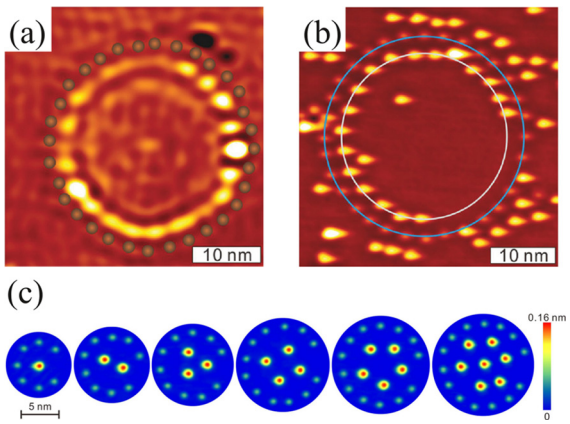

FIG. 2. (a) Statistics on Gd adatom's diffusion inside the Fe corral on Ag(111). (b) Ring-like structure formed upon deposition of more Gd adatoms. Cao *et al.*, Phys. Rev. B **87**, 085415 (2013). Copyright 2013 American Physical Society. (c) Topographies of the quantized Gd-atom trapping in open Fe corrals with different diameters. Cao *et al.*, Phys. Rev. B **90**, 045433 (2014). Copyright 2014 American Physical Society.

Based on the observed higher occupancy probability of atom diffusion in the outmost orbit inside the corral, one can expect that upon increasing the Gd coverage, most of the adatoms will be located near the quantum corral, forming a ring-like structure. Indeed, the experimental observation highlights this effect unambiguously [Fig. 2(b)]. The deposition of more adatoms will make the inner orbits occupied and form an onion-like structure at optimal coverage as predicted theoretically.[25] These atomic structures are different from the self-assembled hexagonal superlattice.[17] Besides the circular nanocorrals, the QSE was also studied in different shaped corrals such as triangular ones and exhibited the ability to control the orientation of the atomic structures.

Therefore, the diffusion behavior and self-assembled structures of adatoms can be significantly modified by introducing the QSE. Since these corrals can also be built by advanced lithography, further combining them with quantum engineering will open possibilities for local functionality design down to the atomic scale.

The statistical fluctuation phenomenon is fundamental and usually unavoidable and can deteriorate the uniformity/reproducibility of the desired atomic structures. As a rule of thumb, the fluctuation scales with the square root of the number of atoms. The smaller the number, the stronger the fluctuation as compared to the total number. For instance, the number of deposited adatoms inside the prepared nanocorrals strongly fluctuates, resulting in a broad distribution of the occupancy histogram.[18,22] In contrast to the conventional closed corrals, Cao *et al.* found that the QSE in open nanocorrals can be used to control the statistical fluctuation of the atomic structures.[18]

Open nanocorrals were built by missing one Fe adatom while keeping the other Fe adatoms on Ag(111) with a separation between 2.0 and 2.5 nm the same as that for the closed corrals. The opening forms a gate to regulate the flow of Gd adatoms traveling in and out, resulting in quantized atom trapping. Depending on the diameters of the open corrals (5–12 nm), one to seven Gd adatoms end up being trapped inside the nanocorrals, preferring to self-arrange in regular polygons [Fig. 2(c)]. A systematic measurement on the number of trapped Gd adatoms as a function of the open-corral diameter has been performed further, for one through seven trapped adatoms except for six. The absence of 6-atom trapping can be understood as follows. As shown in Fig. 2(c), the trapped atoms prefer to form equilateral polygon structures. If an equilateral hexagon is formed by 6 Gd atoms, an additional Gd atom can also be stabilized at the center position of the hexagon since its distance to the surrounding Gd atom is the same as the separation between the surrounding Gd atoms. In such a case, the total energy of forming a 7-atom structure is lower than that of a 6-atom structure plus one atom located outside the corral. The mechanism of this quantized trapping was revealed by STM imaging and energy landscape calculations, which can be

attributed to the QSE induced self-regulating process: when the number of adatoms inside the corral is insufficient, trapping of additional atoms is automatically triggered; whereas if there are too many atoms inside the corral, an efficient overall repulsion process sets in and the extra atoms go out. Remarkably, the wide plateaus of the staircase in the curve of the number of trapped Gd adatoms vs the open-corral diameter illustrate the robustness and stability of this open-corral atom trapping, giving sufficient tolerance for reliable nanostructure design and fabrication via this method.

The effect of controlling the statistical fluctuation utilizing the QSE in open nanocorrals was further illustrated with the direct comparison between open and closed corrals in the context of their trapping capabilities. The statistical histogram for the number of trapped Gd adatoms in an array of open 8.5-nm corrals shows a single value, while a broad distribution in the histogram was found in an array of closed corrals of the same diameter.

These experimental findings demonstrate that the QSE in open nanocorrals can be utilized to enforce a number-selection rule and control the statistical fluctuation of the atomic structures over a wide range of experimentally relevant conditions, whereas closed corrals do not. This method opens a potential way to improve the uniformity/reproducibility of the desired device structures and processes.

The Kondo effect describes the scattering of conduction electrons by the local spin of a magnetic impurity and has inspired many advances of both theories and experiments. One of the continuous motivations to explore that the Kondo effect is the spin control toward spintronic devices. When the system temperature is much lower than the characteristic temperature, i.e., Kondo temperature, the spin of a magnetic impurity will be screened, while the spin remains, when the system temperature is higher than Kondo temperature. In addition, one can also manipulate the spin state of magnetic impurities at ambient temperature by controlling the Kondo temperature. Utilizing the QSE in thin Pb films, the Kondo temperature of the MnPc molecule shows oscillation behavior with the film thickness and can reach a value up to 419 K.[27] For quantum dots, the Kondo temperature can be tuned by means of a gate voltage as a single-particle energy state near the Fermi energy.[28]

Given those studies in both 1D-confined thin films and 3D-confined quantum dots, a natural question of whether the in-plane QSE can modulate the Kondo effect or not arises. The in-plane quantum size effect requires the wave vector to be parallel to the surface. Thus, the surface state comes into the consideration, e.g., the surface state of noble metal with (111) orientation. In fact, whether and how the surface state influences the Kondo temperature have been in hot debate for a certain time.[29–35] This discrepancy is recently solved by the extended experiments, which showed that Kondo temperature of Co adatoms placed at the center of quantum corrals atop Ag(111) [Fig. 3(a)] oscillates strongly as a function of the diameter of the corral.[19] The authors compared the *dI/dV* measurements of the empty corral by removing the Co atom at the center [Fig. 3(b)]. The summarized corral radius *r*-dependent Kondo resonance width *w* in the occupied corral [Fig. 3(c)] and the *dI/dV* signal at the Fermi level measured in the center of the empty corrals [Fig. 3(d)] exhibit similar oscillations. The maximum value of *w* reaches 25.1 meV (corresponding to a Kondo temperature of ∼291 K), which is about three times the value obtained for a single Co monomer on a wide terrace. The oscillation period is ∼3.8 nm, which is consistent with the half Fermi wavelength

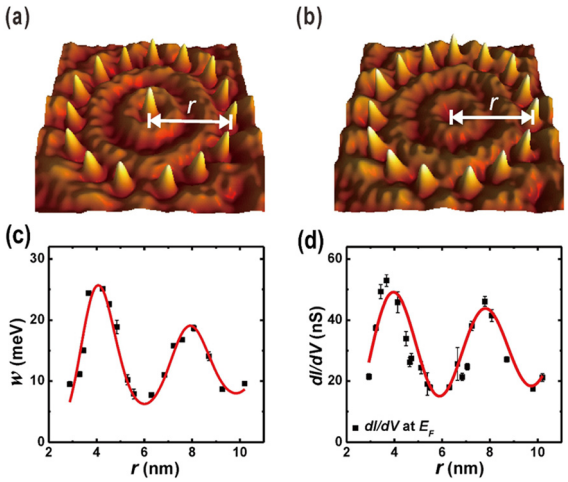

FIG. 3. (a) and (b) show the topographic view of Co-centered and empty quantum corrals with the radius of the nanocorrals, respectively. (c) *r*-dependent Kondo resonance width *w* for the occupied corral. (d) *r*-dependent *dI/dV* at the Fermi level. Red curves in (c) and (d) are fittings. Li *et al.*, Phys. Rev. B **97**, 035417 (2018). Copyright 2018 American Physical Society.

of the Ag(111) surface state. It is generally accepted that the Kondo temperature can be expressed as $k_B T_K = D\exp(-\frac{1}{J\rho(E_F)})$,[27,36] where D is the band cutoff, J is the exchange constant, $\rho(E_F)$ is the local density of state (LDOS) at the Fermi level, and k_B is the Boltzmann constant. The authors extended the expression to accommodate both the bulk and surface states, i.e., two-band contribution with the form of $k_B T_K = \tilde{D}\exp(-\frac{1}{J_b\rho_b(E_F)+J_s\rho_s(E_F)})$, where J_b and J_s are the exchange constants of the adatom with the bulk and surface states, respectively, and $\tilde{D}$ is the effective band cutoff. Fitting the measured Kondo resonance [red curve in Fig. 3(c)] and the extracted LDOS from the *dI/dV* spectrum [red curve in Fig. 3(d)], the exchange values of single adatom with the bulk and surface states, namely, J_b and J_s were obtained.

Moreover, the subsequent works also find site-dependent Kondo temperature for single Co adatom placed at different positions within nanocorrals[37] or on one monolayer Ag-covered Cu(111) surface.[38] Note that the latter surface has surface reconstruction, which confines the surface states to spatially modulated LDOS. Based on these, one may envision an atomic-scale magnetic memory patterned with arrays of paired low-and-high LDOS units via STM lithography or nanofabrication for Co/Ag(111) or Co/1 ML Ag/Cu(111), where the Co adatom at the high LDOS site is nonmagnetic meaning "0" and the one at the low LDOS site is magnetic meaning "1." The writing procedure can be realized through atom manipulation by moving the Co atom from the high LDOS site to the low LDOS site and *vice versa*. The readout can be made via the scanning tunneling microscopy/spectroscopy (STS). Together with the findings in thin films and quantum dots, these observations complement the viable ways to modulate the Kondo effect via the QSE.

The QSE in nanocorrals can also be used to build atomic logic gates. As demonstrated by Manoharan *et al.* in 2000, the Kondo effect-based quantum mirages show great potential in information transport at the nanometer scale.[16] The observed quantum mirages are Kondo

effect based and thus are limited to near the Fermi level only. Recently. Li *et al.*[20] found that a Kondo-free mirage rooted in the inversion effect,[39] which has high signal transport efficiency and can operate in a wide energy range.[20] Taking advantage of these merits, they demonstrate the atomic logic gates of NOT, FANOUT, and OR. In their conceptual design, the input "1"/"0" is the presence/absence of the adatom at one focal point and the output "1"/"0" is the triggered quantum mirages with a high/low difference of *dI/dV* intensity at the other focus. The NOT gate is a two-terminal device, which just corresponds to the two foci of an elliptical quantum corral by utilizing inverted mirage or anti-mirage. To realize FANOUT and OR gates, a special geometry by combining two elliptical quantum corrals with one joint focus was devised to form the three-terminal device [Fig. 4]. The presence/absence of an adatom at joint focus A is as the input "1"/"0" and *dI/dV* intensities at B and C are as the outputs. The *dI/dV* map obtained from "0" input [Fig. 4(a)] at a bias voltage of 34 mV shows low contrast at both foci B and C [Fig. 4(b)], corresponding to "0" outputs. When shifting the input to "1" by placing an Fe adatom at joint focus A [Fig. 4(c)], the corresponding *dI/dV* map [Fig. 4(d)] shows high intensity ("1") at both outputs. The relation between the input and outputs satisfies the function of a FANOUT gate. Besides, an OR gate was also demonstrated when swapping the input and output. We note that the output is sensitive to the chosen bias voltage due to the quantum interference. When a destructive condition is used, input 1 can result in an output 0. This was applied to construct a NOT gate in an elliptical quantum corral.[20]

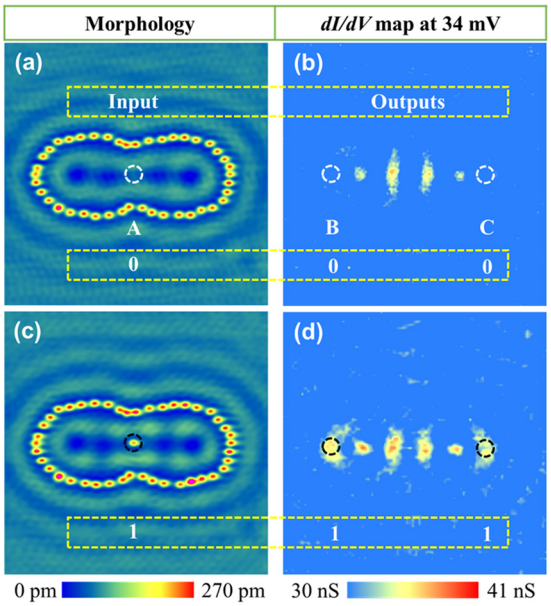

FIG. 4. (a) Topography of a confocal elliptical quantum corral (EQC). Both the EQCs used to build the confocal EQC have the same size of major axis length = 6.6 nm and eccentricity = 0.7. Joint focus A is used as the input, and the other two foci B and C are the outputs. (b) The corresponding *dI/dV* map of panel (a) at the bias voltage of 34 mV. The *dI/dV* values of outputs B and C are 30.2 nS and 31.7 nS, respectively. (c) Topography of the same confocal EQC in panel (a) but with an additional Fe adatom placed at joint focus A. (d) The corresponding *dI/dV* map of panel (c) at the same bias voltage of 34 mV. The *dI/dV* values of outputs B and C are 35.6 nS and 35.2 nS, respectively. Dashed circles mark the focal positions, for which black means 1 and white means 0. Li *et al.*, Nat. Commun. **11**, 1400 (2020). Copyright 2020 Springer Nature.

Although the atomic basic logic gates have been demonstrated, there are still many further explorations need to be done before their applications. First, as discussed in the original work of Li *et al.*,[20] the logic threshold of the on-off signal needs to be improved. As the presence of the bulk state significantly reduces the on-off ratio by contributing as a constant background, seeking a system with a reduced or even vanishing bulk state can achieve a higher on-off ratio. Besides, seeking a system with a strong confinement effect can also enhance the on-off ratio. Furthermore, devices with more than three terminals can also be designed by combining three or four elliptical quantum corrals with one joint focus to form four or five terminals.[40] Finally, one can even envision a structure with cascaded FANOUT or OR gates.

We have discussed the QSE in nanocorrals on noble metal (111) surfaces, from quantum-guided diffusion and self-assembly, to controlling statistical fluctuation, tuning Kondo temperature, and building atomic logic gates. On one hand, noble metal (111) surfaces provide an excellent playground to explore the QSE in nanocorrals and there remains much room to be explored. On the other hand, seeking other potential materials is also highly desired. This effort on noble metal (111) surfaces should be transferrable to the potential materials. Here, we list a few potential candidates that may produce fascinating physical phenomena in the QSE. For example, the topological insulators, which have surface states only near the Fermi level, are good candidates to investigate. A recent work showed that nanocorrals with Rb atoms can be built on the Bi_2Se_3(111) surface and demonstrated the ability to create tailored electronic potential landscapes on topological surfaces with atomic-scale control.[41] As topological insulators are generally topological protected from nonmagnetic impurities, the quantum confinement for nonmagnetic impurities on topological insulators is hard to observe. A recent theoretical prediction, however, showed that magnetic nanocorrals can yield strong spin-polarized quantum well states.[42] This could be probed via the state-of-the-art spin-polarized STM, which shows great capability in resolving complex magnetic structures like magnetic skyrmions.[43,44] Another candidate is the superconductor substrate, which is also considered as the potential candidate for quantum computation and quantum information.[45,46] As aforementioned, the QSE in nanocorrals on the noble metal surface demonstrates the ability of information and logic gates. When taking advantage of the QSE in nanocorrals, it might promote the explorations of quantum computation and quantum information. Actually, a theoretical work has showed the quantum mirage effect for a magnetic adatom on the superconductor substrate confined in a nanocorral.[47] In addition, two-dimensional materials are booming, while the study of the lateral quantum confinement in them is still at an early stage. We believe that those two-dimensional materials such as transitional metal dichalcogenides[48,49] are worth investigating. Finally, we would like to point out that the QSE in nanocorrals is observed under ultrahigh vacuum, which might be too expensive to use commercially. For practical application, one could consider the encapsulation to protect devices from the ambient environment, similar to what has been done in quantum dots.[50]

AUTHORS' CONTRIBUTIONS

Q.L. and R.C. contributed equally to this work.

This work was supported by the National Key R&D Program of China (Grant Nos. 2017YFA0303202 and 2018YFA0306004), the National Natural Science Foundation of China (Grant Nos. 11974165, 51971110, and 11734006), the China Postdoctoral Science Foundation (Grant No. 2019M651766), and the Natural Science Foundation of Jiangsu Province (Grant Nos. BK20190057 and BK20180889).

DATA AVAILABILITY

Data sharing is not applicable to this article as no new data were created or analyzed in this study.

REFERENCES

[1]M. M. Waldrop, Nature **530**, 144 (2016).
[2]V. N. Lutskii, Phys. Status Solidi A **1**, 199 (1970).
[3]Y. F. Ogrin, V. N. Lutskii, and M. I. Elinson, Pis'ma zh. Eksp. Teor. Fiz. **3**, 114 (1966).
[4]V. N. Lutskii, D. N. Korneev, and M. I. Elinson, Pis'ma Zh. Eksp. Teor. Fiz. **4**, 267 (1966).
[5]M. C. Tringides, M. Jałochowski, and E. Bauer, Phys. Today **60**(4), 50 (2007).
[6]M. N. Baibich, J. M. Broto, A. Fert, F. N. Van Dau, F. Petroff, P. Etienne, G. Creuzet, A. Friederich, and J. Chazelas, Phys. Rev. Lett. **61**, 2472 (1988).
[7]G. Binasch, P. Grünberg, F. Saurenbach, and W. Zinn, Phys. Rev. B **39**, 4828(R) (1989).
[8]M. A. Reed, J. N. Randall, R. J. Aggarwal, R. J. Matyi, T. M. Moore, and A. E. Wetsel, Phys. Rev. Lett. **60**, 535 (1988).
[9]N. N. Ledentsov, Semicond. Sci. Technol. **26**, 014001 (2011).
[10]A. Kiani, B. R. Sutherland, Y. Kim, O. Ouellette, L. Levina, G. Walters, C.-T. Dinh, M. Liu, O. Voznyy, X. Lan, A. J. Labelle, A. H. Ip, A. Proppe, G. H. Ahmed, O. F. Mohammed, S. Hoogland, and E. H. Sargent, Appl. Phys. Lett. **109**, 183105 (2016).
[11]K. Yang, F. Li, C. P. Veeramalai, and T. Guo, Appl. Phys. Lett. **110**, 083102 (2017).
[12]S. K. Adams, N. W. Piekiel, M. H. Ervin, and C. J. Morris, Appl. Phys. Lett. **112**, 233108 (2018).
[13]C. S. Lent and P. D. Tougaw, Proc. IEEE **85**, 541 (1997).
[14]D. M. Eigler and E. K. Schweizer, Nature **344**, 524 (1990).
[15]M. F. Crommie, C. P. Lutz, and D. M. Eigler, Science **262**, 218 (1993).
[16]H. C. Manoharan, C. P. Lutz, and D. M. Eigler, Nature **403**, 512 (2000).
[17]R. X. Cao, B. F. Miao, Z. F. Zhong, L. Sun, B. You, W. Zhang, D. Wu, A. Hu, S. D. Bader, and H. F. Ding, Phys. Rev. B **87**, 085415 (2013).
[18]R. X. Cao, Z. Liu, B. F. Miao, L. Sun, D. Wu, B. You, S. C. Li, W. Zhang, A. Hu, S. D. Bader, and H. F. Ding, Phys. Rev. B **90**, 045433 (2014).
[19]Q. L. Li, C. Zheng, R. Wang, B. F. Miao, R. X. Cao, L. Sun, D. Wu, Y. Z. Wu, S. C. Li, B. G. Wang, and H. F. Ding, Phys. Rev. B **97**, 035417 (2018).
[20]Q. L. Li, X. X. Li, B. F. Miao, L. Sun, G. Chen, P. Han, and H. F. Ding, Nat. Commun. **11**, 1400 (2020).
[21]Z. Cheng, J. Wyrick, M. Luo, D. Sun, D. Kim, Y. Zhu, W. Lu, K. Kim, T. L. Einstein, and L. Bartels, Phys. Rev. Lett. **105**, 066104 (2010).
[22]M. Pivetta, G. E. Pacchioni, U. Schlickum, J. V. Barth, and H. Brune, Phys. Rev. Lett. **110**, 086102 (2013).
[23]N. N. Negulyaev, V. S. Stepanyuk, L. Niebergall, P. Bruno, W. Hergert, J. Repp, K. H. Rieder, and G. Meyer, Phys. Rev. Lett. **101**, 226601 (2008).
[24]A. Schiffrin, J. Reichert, W. Auwärter, G. Jahnz, Y. Pennec, A. Weber-Bargioni, V. S. Stepanyuk, L. Niebergall, P. Bruno, and J. V. Barth, Phys. Rev. B **78**, 035424 (2008).
[25]V. S. Stepanyuk, N. N. Negulyaev, L. Niebergall, R. C. Longo, and P. Bruno, Phys. Rev. Lett. **97**, 186403 (2006).
[26]J. Hu, R. X. Cao, B. F. Miao, Z. Liu, Z. F. Zhong, L. Sun, B. You, D. Wu, W. Zhang, A. Hu, S. D. Bader, and H. F. Ding, Surf. Sci. **618**, 148 (2013).
[27]Y. S. Fu, S. H. Ji, X. Chen, X. C. Ma, R. Wu, C. C. Wang, W. H. Duan, X. H. Qiu, B. Sun, P. Zhang, J. F. Jia, and Q. K. Xue, Phys. Rev. Lett. **99**, 256601 (2007).
[28]S. M. Cronenwett, T. H. Oosterkamp, and L. P. Kouwenhoven, Science **281**, 540 (1998).
[29]N. Knorr, M. A. Schneider, L. Diekhöner, P. Wahl, and K. Kern, Phys. Rev. Lett. **88**, 096804 (2002).
[30]L. Limot and R. Berndt, Appl. Surf. Sci. **237**, 576 (2004).
[31]J. Merino and O. Gunnarsson, Phys. Rev. Lett. **93**, 156601 (2004).
[32]C. Y. Lin, A. H. Castro Neto, and B. A. Jones, Phys. Rev. B **71**, 035417 (2005).
[33]M. A. Schneider, P. Wahl, L. Diekhöner, L. Vitali, G. Wittich, and K. Kern, Jpn. J. Appl. Phys. **44**, 5328 (2005).
[34]C. Y. Lin, A. H. Castro Neto, and B. A. Jones, Phys. Rev. Lett. **97**, 156102 (2006).
[35]J. Henzl and K. Morgenstern, Phys. Rev. Lett. **98**, 266601 (2007).
[36]U. Schwingenschlögl and I. A. Shelykh, Phys. Rev. B **80**, 033101 (2009).
[37]Q. L. Li, R. Wang, K. X. Xie, X. X. Li, C. Zheng, R. X. Cao, B. F. Miao, L. Sun, B. G. Wang, and H. F. Ding, Phys. Rev. B **97**, 155401 (2018).
[38]K. X. Xie, Q. L. Li, X. X. Li, B. F. Miao, L. Sun, and H. F. Ding, Surf. Sci. **679**, 74 (2019).
[39]J. Kliewer, R. Berndt, and S. Crampin, Phys. Rev. Lett. **85**, 4936 (2000).
[40]D. M. Eigler, C. P. Lutz, M. F. Crommie, H. C. Manoharan, A. J. Heinrich, and J. A. Gupta, Philos. Trans. R. Soc. London, Ser. A **362**, 1135 (2004).
[41]P. Löptien, L. Zhou, J. Wiebe, A. A. Khajetoorians, J. L. Mi, B. B. Iversen, P. Hofmann, and R. Wiesendanger, Phys. Rev. B **89**, 085401 (2014).
[42]C. Zheng, Q. L. Li, B. F. Miao, L. Sun, R. Wang, X. X. Li, and H. F. Ding, Phys. Rev. B **96**, 235444 (2017).
[43]S. Heinze, K. von Bergmann, M. Menzel, J. Brede, A. Kubetzka, R. Wiesendanger, G. Bihlmayer, and S. Blügel, Nat. Phys. **7**, 713 (2011).
[44]N. Romming, C. Hanneken, M. Menzel, J. E. Bickel, B. Wolter, K. von Bergmann, A. Kubetzka, and R. Wiesendanger, Science **341**, 636 (2013).
[45]F. Arute, K. Arya, R. Babbush, D. Bacon, J. C. Bardin, R. Barends, R. Biswas, S. Boixo, F. G. S. L. Brandao, D. A. Buell, B. Burkett, Y. Chen, Z. Chen, B. Chiaro, R. Collins, W. Courtney, A. Dunsworth, E. Farhi, B. Foxen, A. Fowler, C. Gidney, M. Giustina, R. Graff, K. Guerin, S. Habegger, M. P. Harrigan, M. J. Hartmann, A. Ho, M. Hoffmann, T. Huang, T. S. Humble, S. V. Isakov, E. Jeffrey, Z. Jiang, D. Kafri, K. Kechedzhi, J. Kelly, P. V. Klimov, S. Knysh, A. Korotkov, F. Kostritsa, D. Landhuis, M. Lindmark, E. Lucero, D. Lyakh, S. Mandrà, J. R. McClean, M. McEwen, A. Megrant, X. Mi, K. Michielsen, M. Mohseni, J. Mutus, O. Naaman, M. Neeley, C. Neill, M. Y. Niu, E. Ostby, A. Petukhov, J. C. Platt, C. Quintana, E. G. Rieffel, P. Roushan, N. C. Rubin, D. Sank, K. J. Satzinger, V. Smelyanskiy, K. J. Sung, M. D. Trevithick, A. Vainsencher, B. Villalonga, T. White, Z. J. Yao, P. Yeh, A. Zalcman, H. Neven, and J. M. Martinis, Nature **574**, 505 (2019).
[46]G. Wendin, Rep. Prog. Phys. **80**, 106001 (2017).
[47]D. K. Morr and N. A. Stavropoulos, Phys. Rev. Lett. **92**, 107006 (2004).
[48]Y. H. Yuan, J. Pan, X. T. Wang, Y. Q. Fang, C. L. Song, L. L. Wang, K. He, X. C. Ma, H. J. Zhang, F. Q. Huang, W. Li, and Q. K. Xue, Nat. Phys. **15**, 1046 (2019).
[49]K. Zhao, H. C. Lin, X. Xiao, W. T. Huang, W. Yao, M. Z. Yan, Y. Xing, Q. H. Zhang, Z. X. Li, S. Hoshino, J. Wang, S. Y. Zhou, L. Gu, M. S. Bahramy, H. Yao, N. Nagaosa, Q. K. Xue, K. T. Law, X. Chen, and S. H. Ji, Nat. Phys. **15**, 904 (2019).
[50]A. Fuhrer, M. Füchsle, T. C. G. Reusch, B. Weber, and M. Y. Simmons, Nano Lett. **9**, 707 (2009).